Distinguishing Liquid Solutions With Alcohol Using Electrical Impedance Measurements: Preliminary Study for Food Safety Applications

John Slay, Roman Sotner, *Member, IEEE*, Todd J. Freeborn, *Senior Member, IEEE*, Jan Jerabek, Ladislav Polak, *Member, IEEE*, Jiri Petrzela, and Vojtech Vyplel

***Abstract*—Methods for identifying contaminants in liquids (such as wine) typically require laboratory analyses of samples using precision equipment, which is expensive in terms of both time and required resources. Therefore, there is a need to identify alternative measurement approaches to reduce the cost in terms of equipment, personnel, and time. One sensing approach to characterize liquid properties and potentially identify contaminants is electrical impedance spectroscopy (EIS). In this work, the electrical impedance of 25-mL samples of three solutions with alcohol (plum distillate, isopropyl alcohol, and winter windshield solution) and a control sample of distilled water were measured using a Keysight 4294A. The liquids with alcohol content (plum distillate, isopropyl alcohol, and winter windshield solution) have lower impedance magnitude in the frequency band below 100 kHz, with specific values of 139, 76, and 7 kΩ at 40 Hz, compared to the reference distilled water sample (approximately 315 kΩ). This suggests that solutions with alcohol (and other chemicals) have increased conductivity in comparison to the distilled water and that impedance may be a suitable approach to differentiate liquids with and without contaminants.**

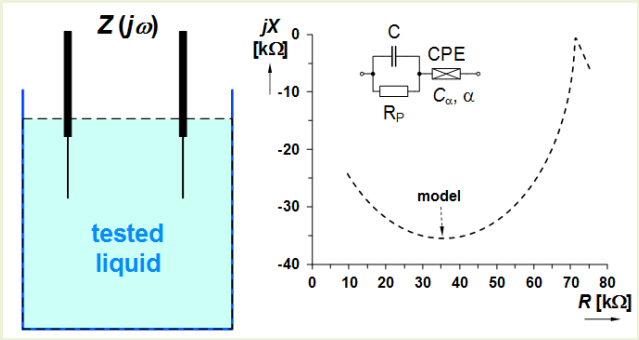

***Index Terms*— Alcohol, Cole-Cole model, electrical impedance spectroscopy (EIS), extraction, impedance analysis, liquids.**

I. Introduction

THE investigation of sensing technologies for monitoring foods and liquids with a specific focus on safety has increased in both attention and importance in recent years. The aim of this line of investigation is to develop techniques to identify contamination accurately and reliably in foods and liquids prior to their sale or consumption to prevent potential illnesses. Recent research has developed electronic sensing systems to emulate the human senses of taste (e.g., electronic tongue) and smell (e.g., electronic nose) to identify and classify food sensory and safety characteristics [1], [2].

Manuscript received 22 August 2023; accepted 12 September 2023. Date of publication 22 September 2023; date of current version 14 November 2023. This work was supported in part by the National Science Foundation under Grant 1951552 and in part by the Czech Science Foundation under Project 23-06070S. The associate editor coordinating the review of this article and approving it for publication was Dr. Prasanta Guha. *(Corresponding author: Roman Sotner.)*

John Slay and Todd J. Freeborn are with the Department of Electrical and Computer Engineering, The University of Alabama, Tuscaloosa, AL 35487 USA (e-mail: JohnRSlayV@outlook.com; tjfreeborn1@eng.ua.edu).

Roman Sotner, Jan Jerabek, Ladislav Polak, Jiri Petrzela, and Vojtech Vyplel are with the Faculty of Electrical Engineering and Communication, Brno University of Technology, 616 00 Brno, Czech Republic (e-mail: sotner@vut.cz; jerabekj@vut.cz; polakl@vut.cz; petrzela@vut.cz).

Digital Object Identifier 10.1109/JSEN.2023.3315798

A. Liquid Analysis and Safety

Sensing techniques focused on evaluating the quality of liquids, such as water, often measure the pH, level, temperature, CO_2, turbidity, humidity [3], and chemical structure [4], [5] of the liquid under test. However, the detailed information of the components within liquid solutions, either intentionally mixed or as an unintentional contaminant, requires the use of sophisticated methods to capture [4], [5]. Typical contaminants of water can be inorganic (e.g., ammonia, arsenic, and chlorine) and organic/biologic (e.g., pesticides, cryptosporidium, and legionella) [4], [5]. Standard methods for identifying these contaminants in water include sample-, sensor placement-, and event detection-based (model-based) methods. For each method, the specific information can be collected using technologies such as: 1) microfluidics sensors; 2) electrical impedance and dielectric impedance spectroscopy; 3) light emission luminescence; 4) infrared spectroscopy;

5) Raman spectroscopy; and 6) biosensors. These methods are often very complex, require expensive and precise measuring equipment, and need highly skilled personnel to complete [4], [5]. Of these methods, impedance-based techniques have the potential for implementation as low-cost, portable equipment, which warrants their further investigation for applications for food and liquid safety.

Dielectric impedance spectroscopy as a technique uses waveguides and the reflection of high-frequency waves to identify the dielectric properties of a material. The variation of the reflective coefficient (phase) of the waveguide (transmission lines) is dependent on both the material dielectric and the applied frequency, with frequency- [6], [7], [8] and time-domain [9] methods frequently used for material testing. This technique has been integrated into test setups to measure liquids in microfluidic channels [10] and combined with thermal sensors to identify liquids using microplate setups [11]. These examples highlight the potential of impedance-based techniques for monitoring liquids. However, often, dielectric impedance spectroscopy utilizes high-frequency (GHz) instruments and interface circuitry for high-frequency operation, which can be challenging to design based on the presence of parasitics and need for impedance-matched interfaces.

An alternative to dielectric impedance spectroscopy is electrical impedance spectroscopy (EIS). This technique measures the frequency-dependent electrical impedance of a material under test (dependent on both the material and the geometry). It is often measured at low frequency (from dc up to tens of megahertz) using simple bipolar or tetrapolar electrode configurations, which reduces the hardware requirements of instruments in comparison to dielectric measurements. While precision impedance instruments are expensive, the commercial availability of integrated circuits that directly measure impedance (e.g., MAX30009 from Maxim Integrated, AD5933 from Analog Devices) is increasing the potential to develop low-cost portable equipment. Applications of impedance sensing for liquids have been investigated for applications, including nitrate concentration monitoring [12], salinity monitoring [13], identification of petroleum and oil (biodiesel) contaminants [14], and monitoring milk adulteration [15]. These highlight the wide range of liquid-focused applications that this technique is being investigated to support. However, there has been little attention focused on the use of electrical impedance-based methods on the measurement of liquid solutions with alcohol (such as wine, beer, and spirits). Recent work by Lopes et al. [16] reported strong correlations between the electrical impedance of wine and chemical properties (e.g., alcohol, acidity, sugars, and density), while van Wyk and Silva [17] reported that impedance measurements could detect *B. bruxellensis* concentrations in wine. While this highlights the success of using impedance-based techniques for measuring wine, these efforts have not investigated if impedance-based techniques can differentiate between wine with and without intentional contaminants.

The existing methods discussed above can be divided into two categories: contact and noncontact, with impedance spectroscopy being a contact-type method. For noninvasive tests with humans or animals, noncontact methods are very advantageous. In our case, food safety aspects are the subject of the experiments. The most significant noncontact methods (dielectric methods) are advantageous in terms of reliability and universality but also require sophisticated hardware, making such measurements very expensive. The advantages of contact methods are their simple sensing readout system (wires), low hardware requirements, and acceptable accuracy for various purposes. Therefore, these systems are more suitable for construction of portable devices than noncontact methods and their expected performance has a great cost/performance ratio.

B. Applications of EIS

Recent developments in the field of EIS [18], [19] have revealed a number of interesting results and consequences regarding the behavior of many biomedical, organic, and inorganic (liquid or solid state) substances. Specific types of inorganic materials and metals are examples of solid-state substances where EIS methodology has received attention in recent years (fabrication of silicon substrates [20] and effects in metal layer-based batteries [21]). A special area of EIS in organic substances deals with analysis and modeling of fruit [22], [23], vegetable [24], [25], and oils [26] as important agricultural products. Also, plant cells, structures, and tissues have received some attention [27], [28]. Impedance spectroscopy serves to assess the quality of agricultural products, including vegetable production [29], [30] and livestock (meat [31], [32], [33]). The effects of temperature [15] were observed and analyzed together with the change in the state of matter visible in the impedance profile (also called impedance signature). EIS was used to monitor long-term plant growth [34] and moisture content during dehydration of vegetables [35]. It has also found importance in medicine [36], human tissue modeling [37], [38], [39], and human skin modeling [40], [41]. However, it appears that only limited attention has been paid to different fluids [42]. Considerable effort has been devoted to modeling the impedance images of various materials and substances to determine suitable models, especially electrical models in the form of electronic circuits [43], [44], [45].

A well-known alcoholic liquid (plum distillate) is a distillation product of the blue plum and important export of the south Moravia region in the Czech Republic (called “slivovice” in the Czech language). This product was the subject of widespread counterfeiting in 2012 with authorities reporting that counterfeit products were created from the mixing for substitution of the plum distillate by methyl alcohol (used in low-cost winter windshield concentrate for cars) [46]. The identification of counterfeit products in this case is challenging because all products require analysis to identify features to classify them as counterfeit. Standard methods for chemical analysis for this purpose are resource intensive both in terms of the required effort for collecting and sending samples to professional laboratories and the expertise to analyze samples using laboratory instruments (e.g., chromatography). Furthermore, this challenge has a significant time pressure because counterfeit products with methyl alcohol are hazardous to human health if consumed, so they must be identified and removed quickly to prevent harm. An optical method, Raman

spectroscopy [47], is another technique for chemical analysis with commercially available portable equipment, but these instruments are still extremely expensive (more than U.S. $10k). Therefore, there is a need for reliable and low-cost methods for immediate identification of dangerous or toxic substances in commercial goods that are for sale for consumption. Impedance spectroscopy has the potential to meet this need as it can be relatively low cost (depending on the instrument) and provides details of the passive electrical properties, which are expected to be different based on the chemical properties of a liquid. While this technique does not provide a complex chemical analysis of a sample, it may have the potential to classify counterfeit liquids (even if it cannot identify the underlying chemical differences). This provides the motivation for this work, to investigate impedance spectroscopy as a method to differentiate between liquid samples of varying alcohol content.

The specific research question that drives this work is: are there differences in the electrical impedance of liquid samples with different alcohol concentrations and different alcohol contents? To answer this study question, the electrical impedance of four liquids (distilled water, plum distillate, isopropyl alcohol, and windshield concentrate) was collected using a precision impedance analyzer and fit to electrical equivalent circuits to facilitate their comparison. The novelty and contributions of our work are given as follows:

1) reporting of impedance profiles of specific alcohol-based samples obtained by identical measurement arrangement and test conditions;
2) presentation and evaluation of equivalent circuit models to accurately represent the frequency-dependent electrical impedance of specific alcohol-based samples measured in a bipolar configuration;
3) comparative study of electrical features of the measured liquid samples to identify characteristics to differentiate samples with different alcohol contents and contaminants.

This article is organized as follows. Section II shows the method of measurement, results, and electrical models of selected samples of liquids (water, plum distillate, isopropyl alcohol, and winter windshield concentrate). Section III contains the comparison and discussion of the obtained results. Next, it includes parameters found from the analyzed results and provides the evaluation of our observations. Section IV concludes this work.

II. Measurement and Impedance Analysis of Selected Liquid Samples

The electrical impedance of all liquid samples in this study was collected using a Keysight (formerly Agilent) 4294A precision impedance analyzer in a two-probe (or bipolar) measurement configuration. This instrument uses a stepped-sine measurement method, where a single sinusoidal voltage or current excitation is applied to the sample under test. The response of the sample at this specific frequency is then measured and the impedance ($Z = V/I$) is calculated using the current through the sample (I) and the voltage across it (V). This process is repeated for multiple frequencies until

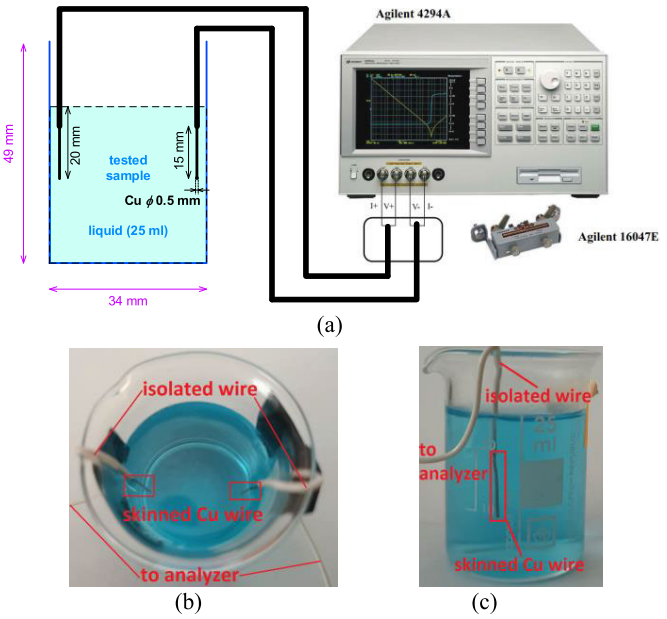

Fig. 1. Measurement setup for liquid impedance analysis. (a) Two-port interconnection to impedance analyzer. (b) Top-view photograph of real sample (beaker). (c) Side-view photograph of beaker.

the total number of frequency points between the upper and lower frequency bounds has been measured. A multifrequency approach is adopted because single-frequency measurements are not sufficient to distinguish samples accurately. Many previous works suggest wideband measurements rather than narrowband tests, mainly due to the accurate representation of the measured results by electrical models [43], [44], [45].

In this work, each liquid sample had a 25-mL volume and was contained in a glass beaker (producer TECHNOSKLO) for the measurement period. Between measurements of different samples, the beaker was flushed with distilled water and dried using a paper towel to remove any residual liquid volumes from influencing future measurements. To interface the impedance analyzer and the liquid sample, two wire electrodes (copper wires with 0.5 mm diameter) were placed into the liquid on one end and the Agilent 16047E interface of the instrument. The wires were inserted to a depth of 20 mm from the liquid surface with an exposed (nonisolated) length of 15 mm. The total length of the cable from the beaker to the measuring instrument was 150 mm. This measurement configuration is shown in Fig. 1(a) for reference with an example of the electrodes placed in the liquid when contained in a beaker given in Fig. 1(b) and (c). All measurements were collected at room temperature. The particular arrangement of electrodes (e.g., material, exposed surface area, distance between electrodes, and depth of immersion in liquid) is expected to impact the measured electrical impedance of the sample. Previous efforts by Freeborn et al. [48], [49], and [50] reported changes in biological tissue impedance based on these factors. As such, the configuration utilized for each sample in this study was fixed to facilitate comparisons between measurements from different samples. The liquid samples were measured across the frequency range from 40 Hz to 2 MHz. The optimum operating band (band of significant change in the sample) is

dependent on both the liquid under test and the experimental setup (e.g., measuring device, cabling, and electrodes). Based on previous works and discussed limitations, the operating band is targeted from low frequency (40 Hz) up to 2 MHz in this work for measurements to capture the characteristics of the electrode/liquid interface and liquid characteristics. While higher frequencies can be collected by the Keysight E4294A, they were not measured in this work as they are typically dominated by parasitics in the measurement configuration and are not representative of the sample. In addition, commercially available impedance measurement integrated circuits have frequency ranges not exceeding 1 MHz; therefore, 40 Hz–2 MHz is appropriate to evaluate for sensitivity to differences in the studied liquids with the ultimate aim of developing portable instrumentation for food safety applications. The applied level of effective (rms) voltage was 10 mV (rules of small-signal modeling). The collected impedance data were saved by the instrument in the magnitude/phase format and stored for later postprocessing. It is important to note that in the two-probe measurement configuration, the electrical impedance reported by the Agilent 4294A represents the impedance of both the electrode/liquid interface and the liquid between the probes.

A. Representation of Impedance Using Equivalent Electrical Circuits

As noted previously, the electrical impedance measurements collected from each liquid sample are composed of data points at multiple frequencies. Using this approach, the frequency dependence of the sample impedance can be observed. Traditional approaches to comparing impedance datasets collected from different samples or at different time points either compare discrete frequencies directly or compare parameter values of equivalent electrical circuits representing the complete range of data. Using the equivalent electrical circuit approach, a circuit topology appropriate to model the "shape" of the data is selected, and then, component values are identified to best fit the impedance of the circuit model to the experimental data (often using numerical optimization methods). One electrical equivalent circuit model that is widely used to represent materials and biological tissues is referred to as the Cole-impedance model [43], [44], [45] and is given in Fig. 2. The Cole-impedance model is a three-element model with two resistors (R_∞ and R_P) and one fractional-order capacitor (C_α). Fractional-order capacitors are theoretical elements with voltage/current characteristics defined by a fractional-order differential equation and are often referred to as constant phase elements (CPEs) [51]. This name is in reference to the phase angle of these devices that are constant with frequency (but lower different than the $-90°$ phase of traditional capacitors). The impedance of a CPE is defined as $Z_{\text{CPE}}(s) = 1/s^\alpha C_\alpha$, where α is the fractional order (between 0 and 1) and C_α is the equivalent capacity [F·sec$^{1-\alpha}$]. The overall impedance of the Cole-impedance model is given by

$$Z_{\text{cole}}(s) = R_\infty + \frac{1}{s^\alpha C_\alpha + \frac{1}{R_P}}. \tag{1}$$

Given an experimental dataset, the Cole-impedance parameters can be found using characteristics from the Nyquist plot

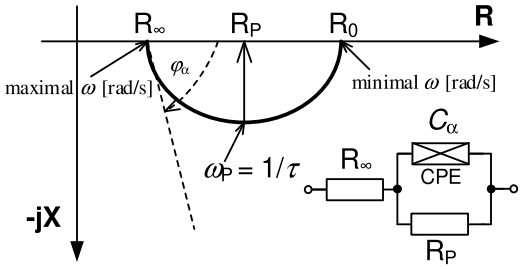

Fig. 2. Basic explanation of the simplest Cole–Cole model (electrochemical circle).

representation (a sample of which is given in Fig. 2). The resistive elements of the model can be determined using the resistance at 0 Hz ($R_0 = R_\infty + R_P$) and resistance at a very high, ideally infinite, frequency (R_∞). These values on the Nyquist plot are shown in Fig. 2 where the sample data intercepts the x-axis. The order of the CPE can be found using $\varphi_\alpha = \alpha\pi/2$ and the value C_α can be determined from the time constant related to the frequency at which the reactance reaches its maximum value ($\omega_P = 1/\tau$), also shown in Fig. 2. Then, the frequency ω_P can be expressed as

$$\omega_P = \frac{1}{\tau} = \frac{1}{(R_P C_\alpha)^{\frac{1}{\alpha}}}. \tag{2}$$

Finally, the value of C_α can be expressed as

$$C_\alpha = \frac{1}{R_P\,(\omega_P)^\alpha}. \tag{3}$$

While the Cole-impedance model can represent the electrical impedance of materials when they exhibit the semiarc characteristics shown in Fig. 2, not all experimental datasets have this characteristic. Complex materials may have multiple semiarcs (which can be modeled with additional R-CPE or CPE terms [45]). Also, while parameters can be determined using the hand-calculation process previously described, they can be estimated by numerical search methods applied to the frequency domain [44], [45], [52], [53], [54] and time domain [55], [56] data. In this work, the NOVA 2.1.6 extraction tool [57] was used to estimate the circuit parameters in the topologies selected to model the experimental data.

B. Distilled Water

The experimental electrical impedance of the distilled water sample is given in Fig. 3(a), with magnitude and phase components given. Furthermore, the Nyquist representation is also shown. Note that the Nyquist plot matches the shape (semiarc) expected of data that can be modeled using the Cole-impedance model [43], [44], [45] and also previously observed for distilled water [58]. The NOVA estimated Cole-model parameters for this experimental data are given in Fig. 4(a). Note that the CPE has been replaced by a traditional capacitor ($\alpha = 1$), supporting that this liquid is well modeled without a fractional-order term. The simulated impedance data using the parameters from Fig. 4(a) are shown in Fig. 3(a) as black dashed lines. Both experimental and simulated data show good visual

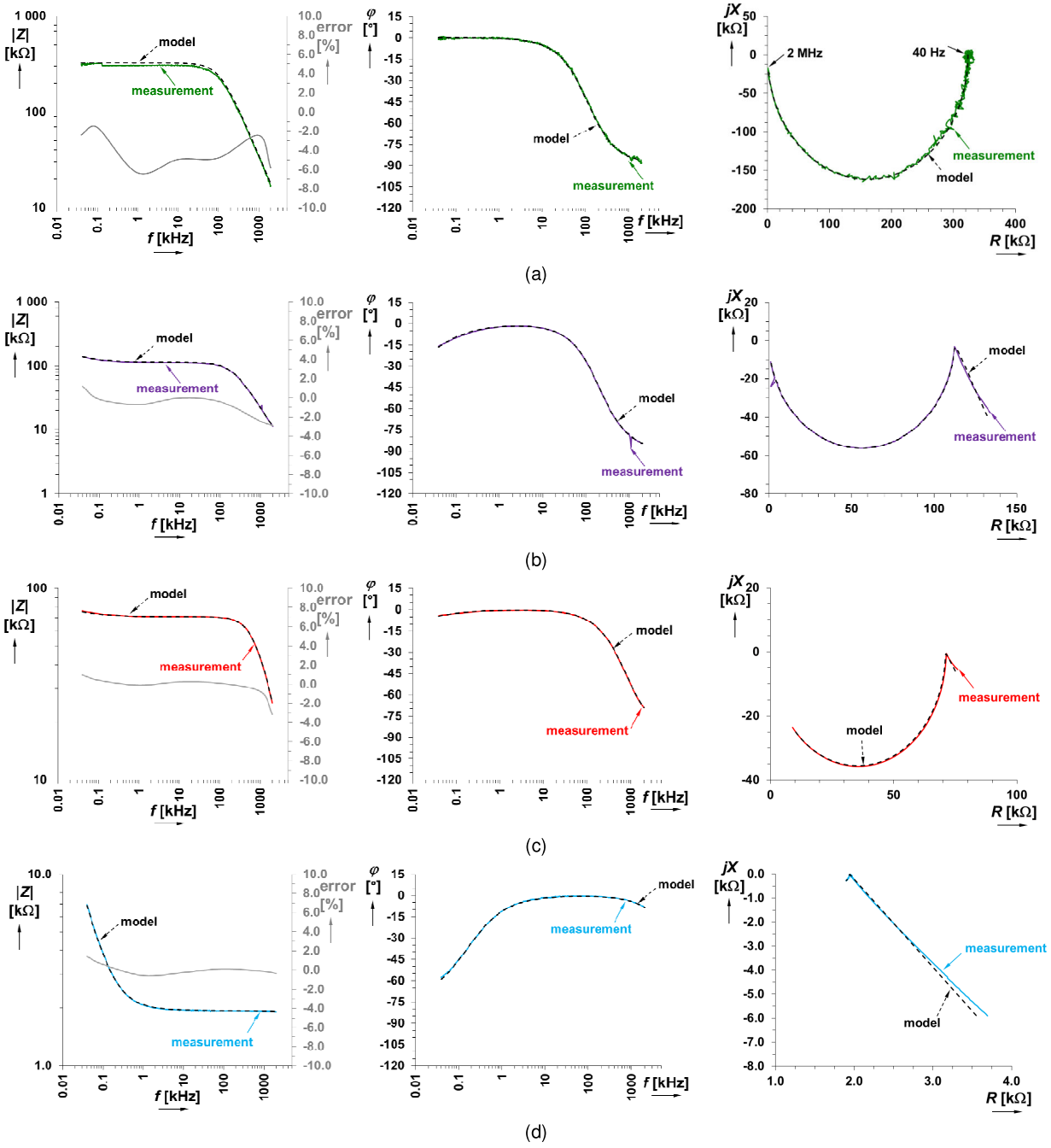

Fig. 3. Analyzed impedance of different liquid samples in magnitude plot (left), argument plot (middle), and Nyquist plot (right). (a) Distilled water. (b) Plum distillate. (c) Isopropyl alcohol. (d) Winter windshield concentrate.

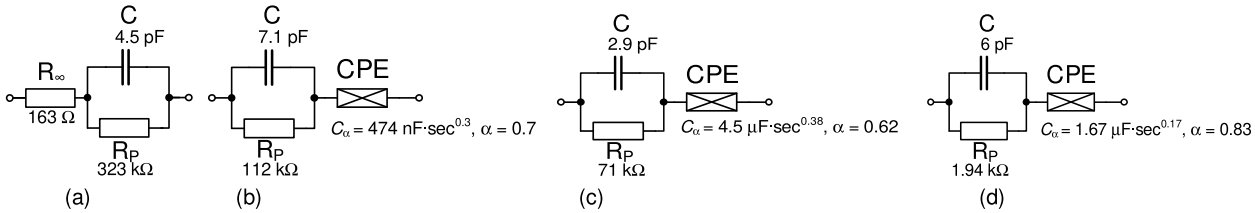

Fig. 4. Extracted circuit models. (a) *R*C equivalent model of distilled water. (b) *R*-*C*-CPE model of plum distillate. (c) Equivalent *R*-*C*-CPE model of isopropyl-alcohol. (d) Equivalent *R*-*C*-CPE model of winter windshield concentrate.

agreement, with relative differences of 2%–4% across the measured frequency range. This measurement serves as a reference against which other samples will be compared (see Table I).

C. Alcohol Plum Distillate

The electrical impedance of the plum distillate, with an alcohol (ethanol) concentration of approximately 38% (the water content is almost 62% and the other constituents are less

TABLE I
QUALITATIVE COMPARISON OF THE OBTAINED RESULTS

Analyzed sample	distilled water	plum distillate (38%)	isopropyl alcohol (95%)	winter windshield concentrate (45%)
Low-frequency impedance magnitude $\|Z_0\|$ (@ 40 Hz) [kΩ]	315	139	76	7
High-frequency impedance magnitude $\|Z_\infty\|$ (@ 2 MHz) [kΩ]	17	11	25.2	1.91
Initial resistance R_0 (@ 40 Hz) [kΩ]	334	134	76	3.7
Final resistance R_∞ (@ 2 MHz) [kΩ]	0.68	1.06	8.91	1.90
Initial phase value (@ 40 Hz) [°]	−1.3	−15.7	−4.2	−57.7
Final phase value (@ 2 MHz) [°]	−87.4	−84.5	−69.4	−8.6
Type of model by used elements	R-C	R-C-CPE	R-C-CPE	R-C-CPE
Response type and frequency location of the most significant differences of samples	Phase (low frequencies)	Phase (low frequencies)	Phase (low frequencies)	magnitude and phase (very significant at low frequencies)
Maximal error of the extracted model in full frequency range [%]	−6	−3	−3	+1.4

TABLE II
COMPARISON OF *R-C*-CPE EQUIVALENT MODEL PARAMETERS ESTIMATED FROM ALCOHOL-BASED LIQUID SAMPLES

model	plum distillate (Fig. 3(b))	isopropyl alcohol (Fig. 3(c))	winter windshield concentrate (Fig. 3(d))
R [kΩ]	112	71	1.94
C [pF]	7.1	2.9	6
C_α [F·sec$^{1-\alpha}$]	474 n	4.5 µ	1.67 µ
α [-]	0.70	0.62	0.83
f_{p2} [kHz]	200	773	13 673
f_{z1} [Hz]	10.6	1	159

than 1%), is given in Fig. 3(b). Note that the low-frequency magnitude is not constant but increases as frequency decreases. Similar low-frequency behavior with decreasing phase angle is also observed. These trends indicate capacitive low-frequency behavior that is not captured by the Cole-model impedance. As a result, an alternative electrical equivalent circuit [shown in Fig. 4(b)] was used to fit these data. This alternative model replaces R_∞ with a CPE. Using NOVA, the estimated parameter values that best fit the plum distillate experimental data to the model in Fig. 4(b) are also listed in this figure. The symbolical impedance of the circuit in Fig. 4(b) is given by

$$Z_{\text{plum}}(s) = \frac{1}{s^\alpha C_\alpha} + \frac{1}{sC + \frac{1}{R_P}}. \tag{4}$$

Simulations using (4) with the estimated parameter values are given in Fig. 3(b) as dashed lines for comparison against the experimental values. The simulations show very good agreement with the experimental data, with <3% relative differences for the magnitude across the measured frequency band. To support further insights into the model impedance, (4) can be modified to the form

$$Z_{\text{plum}}(s) = \frac{(C + C_\alpha)\, s^\alpha + \frac{1}{R_P}}{C_\alpha s^\alpha \left(sC + \frac{1}{R_P}\right)} = \frac{\left(s^{1-\alpha} + \frac{C_\alpha}{C}\right)\left(s^\alpha + \frac{1}{C_\alpha R_P}\right)}{C_\alpha s^\alpha \left(sC + \frac{1}{R_P}\right)} \tag{5}$$

where the equation poles can by identified at $\omega_{p1} = 0$ Hz and $\omega_{p2} = 1/(R_P C_P)$. The equation zeros are located at

$$\omega_{z1} = \left(\frac{1}{R_P C_\alpha}\right)^{\frac{1}{\alpha}} \tag{6}$$

and

$$\omega_{z2} = \left(\frac{C_\alpha}{C}\right)^{\frac{1}{1-\alpha}}. \tag{7}$$

This model has a pole at the origin (0 Hz), which contributes to the increasing impedance magnitude with decreasing frequency. The second pole frequency calculated using $f_{p2} = 1/(2\pi R_P C_P)$ with the values given in Fig. 4(b) is $f_{p2} = 200$ kHz. Using (6) and (7) with the NOVA extracted model values, $f_{z1} = 10.6$ Hz and f_{z2} has a very high (nearly infinite value). Further evaluation of these parameters is provided for all tested alcohol-based samples in Table II. In our case, the theoretical low-frequency resistance R_0 has infinite value [see Fig. 4(b)]. The magnitude of impedance goes to 0 for high frequencies (defined only by the CPE behavior). Note that the validity of the symbolical equations presented for these frequencies is limited for $\alpha > 0.3$.

D. Isopropyl Alcohol

The electrical impedance (presented in magnitude, phase, and Nyquist formats) of liquid isopropyl alcohol with a concentration of 95% is given in Fig. 3(c). Similar to the plum distillate measurements, the low-frequency behavior is not constant (which was observed for distilled water) but has increasing magnitude/decreasing phase angle with decreasing frequency. This supports the use of the model in Fig. 4(c) (used to initially fit the plum distillate data) to also fit the isopropyl-alcohol data. The NOVA estimated parameters that best fit the experimental data from Fig. 3(c) to the model in Fig. 4(c) are also listed in Fig. 4(c). Simulations of (4) using these parameters are given in Fig. 3(c) as dashed lines for comparison. They show good visual agreement with the

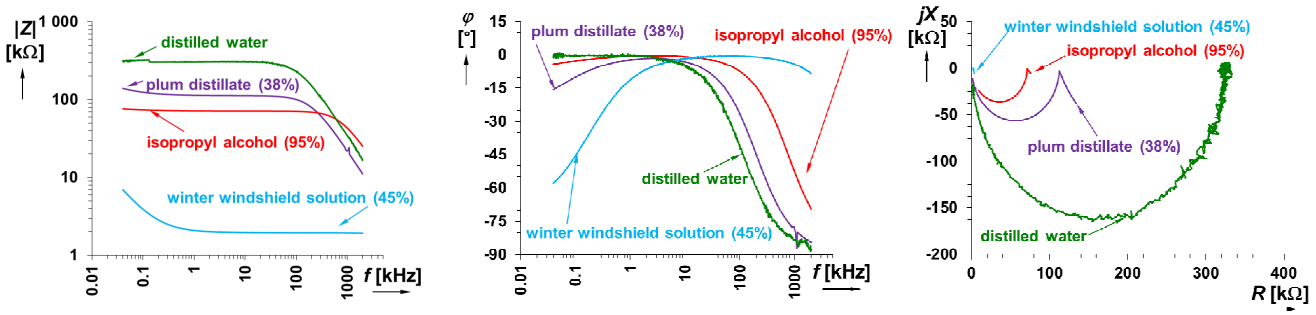

(a) (b) (c)

Fig. 5. Comparison of all analyzed samples. (a) Magnitude plot. (b) Argument plot. (c) Nyquist plot.

experimental data, with less than 3% relative differences across the measured frequency band.

E. Winter Windshield Concentrate

The electrical impedance (presented in magnitude, phase, and Nyquist formats) of winter windshield concentrate (a solution with methyl alcohol and other potentially toxic chemicals) is given in Fig. 3(d). For this experiment, the specific brand Aroso (for −30 °C) from the company Aroso-Vertriebs GmbH was tested (it was selected as a convenience sample for this initial study). The concentration of alcohol and additional components is not presented on the labeling of this product. Simple measurement of alcohol concentration by hydrometer tester shows a value of 45%. In comparison to the other measured liquids, the winter windshield concentrate has the largest increase in impedance magnitude and decrease in phase angle at low frequencies and also generally the lowest impedance magnitude from all measured samples. These characteristics are still well-modeled by the equivalent electrical circuit given in Fig. 4(d) and fit previously to the other solutions with alcohol content. The NOVA estimated parameters of the R-C-CPE model that best fit the experimental data in Fig. 3(d) are detailed in Fig. 4(d). Simulations using these values in (4) are given in Fig. 3(d) as dashed lines. The relative difference between simulations of the equivalent model and the experimental measurements does not exceed 1.4% over the measured frequency band.

III. Comparison Measured Samples and Extracted Equivalent Models

To compare the electrical impedance measurements of the four liquid samples, the magnitude, phase, and Nyquist representations of each are given in Fig. 5. From Fig. 5(a), all liquids with alcohol content (plum distillate, isopropyl alcohol, and winter windshield solution) have lower impedance magnitude in the frequency band below 100 kHz compared to the reference distilled water sample. A lower impedance magnitude suggests that solutions with alcohol (and other chemicals) have increased conductivity in comparison to the distilled water, expected to be a result of greater numbers of charge carriers (e.g., ions) in the solutions. The low-frequency increase of magnitude and the low-frequency decrease of phase angle observed for solutions with alcohol (compared to the reference distilled water) also suggest that there are electrode/liquid interactions between ions not present in distilled water dominating the low-frequency characteristics of the other samples. The mechanisms of these differences are outside the scope of this work, but further research is recommended to identify what electrochemical interactions drive this impedance behavior (and to determine whether it may be a potential indicator of alcohol concentration/content).

The differences in impedance magnitude/phase between samples are also clearly observed visually as differences in the semiarc radius and projected x-axis intercepts (representing the resistances at low/high frequencies) of the Nyquist plots in Fig. 5(c). Compared to the distilled water sample, all samples with alcohol in this study have a smaller semiarc radius than the distilled water. A summary of the qualitative features estimated from the experimental results for further comparison is provided in Table I.

Next, Table II summarizes the circuit model parameters estimated using NOVA from the experimental impedance of the alcoholic liquids. The frequency values f_{p2} and f_{z1} are in reference to the symbolical model impedance and poles/zeros of (5). From the simulation data presented in Fig. 3, the circuit models and the estimated parameters well represent the liquids in this study showing less than 6% relative impedance magnitude differences across all samples.

The differences in the R-C-CPE parameters also reflect the trends that are observed in the experimental datasets. Specifically, the decrease in impedance magnitude between samples is reflected in the R (R_P respectively) parameter with values of 112, 71, and 1.94 kΩ for the plum distillate, isopropyl alcohol, and winter windshield concentrate, respectively. Again, this is expected to reflect the increase in ions (or a difference in ion species) serving as charge carriers in the solution. While there are differences in the other parameters between solutions, there is not a clear trend with which to classify the solutions.

Overall, this preliminary study supports that there are differences in electrical impedance (and the resulting circuit model parameters to represent this impedance) between the liquid samples in this study. Specifically, the observed impedance magnitude decreases compared to the reference measurement of distilled water are attributed to the alcohol content/concentration in the measured samples. All samples with alcohol had an impedance magnitude (at 40 Hz) of 170 kΩ or lower than distilled water. Furthermore, samples of

isopropyl alcohol and winter windshield concentrate both had higher concentrations than the plum distillate. This suggests that the addition of liquids (such as isopropyl alcohol or the windshield concentrate) to plum distillate would decrease the impedance magnitude characteristics and could serve as an indicator of the plum distillate being genuine or counterfeit/contaminated. This has the potential to increase the availability of methods to quickly test liquids in real-world environments if this method can be translated to a low-cost portable device (highlighting future avenues for this research). Advantages of this electrical impedance focused method are: 1) fast measurement and short evaluation time; 2) possibly low cost; 3) simple; and 4) sufficiently selective (evident difference of winter concentrate from other alcohols). Disadvantages of the proposed concept are: 1) lower accuracy than in the case of Raman spectroscopy; 2) identical arrangement and placement of electrodes required for each measurement, their distance, exposited depth, and so on (the measuring setup must be identical in all cases); and 3) impedance profiles of liquids similar alcohol concentrations may be difficult to distinguish, all of which require further research to investigate but highlight the direction of research necessary to continue advancing understanding of this topic and its translation into portable equipment for liquid assessment/quality testing.

IV. Conclusion

This work supports that the electrical impedance characteristic of liquid samples may have potential applications for the classification of liquids with alcohol as genuine or counterfeit (with potential classification of the type of contaminant as life threatening). The dangerous windshield winter concentrate sample in this work had the most significant magnitude difference compared to the other samples. The impedance plots generated from the experimental data in this work indicate that the concentration of alcohol (and also other chemical components in the samples) creates some systematical difference (decreasing magnitude, decreasing radius of circles of Nyquist plot, and high-frequency phase response drop). However, future work is required to evaluate whether these differences are consistent across samples measured at different times and from different manufacturers, to identify clear thresholds or algorithmic identification approaches to classify liquids, and to develop low-cost portable equipment that can easily implement this identification process in real-world settings.

The methods presented in [59] and [60] show highly selective measurements compared to our wideband low- and middle-range frequency bands. The methods discussed are aimed at noncontact (noninvasive) human blood analysis, in particular glucose concentration monitoring [59], considering the presence of alcohol concentration [60]. In our case, the principle of the method requires the evaluation of a wider range of frequencies and impedances for the extraction of electrical model parameters. In addition, the contact (invasive) measurement is acceptable in our case because our experiments do not involve humans or animals, but food safety aspects.

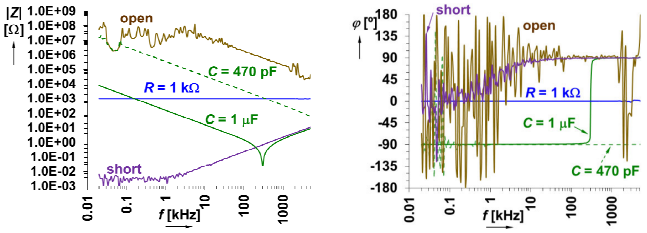

Fig. 6. Measurement by calibrated analyzer and setup (open, short) showing exemplary samples of typical real resistance (resistor) and real reactance (capacitors). (a) Magnitude of impedance. (b) Phase of impedance.

The electrical components necessary for a portable impedance measurement device (e.g., a specific integrated circuit for impedance measurement, a control unit, display, and auxiliary elements mentioned in Section I) are all commercially available with potential to be integrated into the mechanical packaging to hold liquid samples for portable testing. With such a portable instrument, the amount of liquid, the distance between the electrodes, and other technical details can be carefully fixed to improve the repeatability and precision of the measurement for use in field environments where samples for food safety need to be captured (beyond tightly controlled laboratory conditions).

Appendix

Calibrated Measurement of Reference Impedance Samples

The experimental results of the distilled water sample shown in Fig. 3(a) are considered as the reference sample for comparison with the alcoholic substances presented in this article. Prior to the collection of any measurements, the Keysight 4294A was calibrated using the open/short procedure to reduce the effect of the Agilent 16047E interface on the measurements. A sample of the open/short measurements from this procedure and the measured values of discrete components (1-kΩ resistor, and 470-pF and 1-μF capacitors) measured after calibration are shown in Fig. 6.

Acknowledgment

Any opinions, findings, conclusions, or recommendations expressed in this material are those of the author(s) and do not necessarily reflect the views of the National Science Foundation.

References

[1] H. Jiang, M. Zhang, B. Bhandari, and B. Adhikari, "Application of electronic tongue for fresh foods quality evaluation: A review," *Food Rev. Int.*, vol. 34, no. 8, pp. 746–769, Jan. 2018, doi: 10.1080/87559129.2018.1424184.

[2] J. Tan and J. Xu, "Applications of electronic nose (e-nose) and electronic tongue (e-tongue) in food quality-related properties determination: A review," *Artif. Intell. Agricult.*, vol. 4, pp. 104–115, 2020, doi: 10.1016/j.aiia.2020.06.003.

[3] S. Konde and S. Deosarkar, "IoT based water quality monitoring system," in *Proc. 2nd Int. Conf. Commun. Inf. Process. (ICCIP)*, 2020, pp. 1–11, doi: 10.2139/ssrn.3645467.

[4] S. N. Zulkifli, H. A. Rahim, and W.-J. Lau, "Detection of contaminants in water supply: A review on state-of-the-art monitoring technologies and their applications," *Sens. Actuators B, Chem.*, vol. 255, pp. 2657–2689, Feb. 2018, doi: 10.1016/j.snb.2017.09.078.

[5] V. D. Krishna, K. Wu, D. Su, M. C. J. Cheeran, J.-P. Wang, and A. Perez, "Nanotechnology: Review of concepts and potential application of sensing platforms in food safety," *Food Microbiol.*, vol. 75, pp. 47–54, Oct. 2018, doi: 10.1016/j.fm.2018.01.025.

[6] L. Su, J. Muñoz-Enano, P. Vélez, P. Casacuberta, M. Gil, and F. Martín, "Phase-variation microwave sensor for permittivity measurements based on a high-impedance half-wavelength transmission line," *IEEE Sensors J.*, vol. 21, no. 9, pp. 10647–10656, May 2021, doi: 10.1109/JSEN.2021.3063112.

[7] L. Su, J. Muñoz-Enano, P. Velez, P. C. Orta, M. Gil, and F. Martin, "Highly sensitive phase variation sensors based on step-impedance coplanar waveguide (CPW) transmission lines," *IEEE Sensors J.*, vol. 21, no. 3, pp. 2864–2872, Feb. 2021, doi: 10.1109/JSEN.2020.3023848.

[8] I. Piekarz, J. Sorocki, K. Wincza, and S. Gruszczynski, "Liquids permittivity measurement using two-wire transmission line sensor," *IEEE Sensors J.*, vol. 18, no. 18, pp. 7458–7466, Sep. 2018, doi: 10.1109/JSEN.2018.2856889.

[9] S. Saeedi and S. Chamaani, "Non-contact time domain ultra wide band milk spectroscopy," *IEEE Sensors J.*, vol. 21, no. 12, pp. 13849–13857, Jun. 2021, doi: 10.1109/JSEN.2021.3068778.

[10] A. E. Omer et al., "Multiple-cell microfluidic dielectric resonator for liquid sensing applications," *IEEE Sensors J.*, vol. 21, no. 5, pp. 6094–6104, Mar. 2021, doi: 10.1109/JSEN.2020.3041700.

[11] J. Goossens et al., "Liquid identification in a microplate format based on thermal and electrical sensor data fusion," *IEEE Sensors J.*, vol. 22, no. 20, pp. 19809–19817, Oct. 2022, doi: 10.1109/JSEN.2022.3202691.

[12] M. E. E. E. Alahi, N. Pereira-Ishak, S. C. Mukhopadhyay, and L. Burkitt, "An Internet-of-Things enabled smart sensing system for nitrate monitoring," *IEEE Internet Things J.*, vol. 5, no. 6, pp. 4409–4417, Dec. 2018, doi: 10.1109/JIOT.2018.2809669.

[13] M. Grossi, C. Parolin, B. Vitali, and B. Riccò, "Electrical impedance spectroscopy (EIS) characterization of saline solutions with a low-cost portable measurement system," *Eng. Sci. Technol., Int. J.*, vol. 22, no. 1, pp. 102–108, Feb. 2019, doi: 10.1016/j.jestch.2018.08.012.

[14] J. R. Delfino et al., "A simple and fast method to determine water content in biodiesel by electrochemical impedance spectroscopy," *Talanta*, vol. 179, pp. 753–759, Mar. 2018, doi: 10.1016/j.talanta.2017.11.053.

[15] G. Durante, W. Becari, F. A. S. Lima, and H. E. M. Peres, "Electrical impedance sensor for real-time detection of bovine milk adulteration," *IEEE Sensors J.*, vol. 16, no. 4, pp. 861–865, Feb. 2016, doi: 10.1109/JSEN.2015.2494624.

[16] A. M. Lopes, J. A. T. Machado, and E. Ramalho, "On the fractional-order modeling of wine," *Eur. Food Res. Technol.*, vol. 243, no. 6, pp. 921–929, Jun. 2017, doi: 10.1007/s00217-016-2806-x.

[17] S. van Wyk and F. Silva, "Enumeration of *Brettanomyces* in wine using impedance," *Appl. Microbiol.*, vol. 1, no. 2, pp. 352–360, Aug. 2021, doi: 10.3390/applmicrobiol1020024.

[18] S. Wang, J. Zhang, O. Gharbi, V. Vivier, M. Gao, and M. E. Orazem, "Electrochemical impedance spectroscopy," *Nature Rev. Methods Primers*, vol. 1, no. 1, pp. 207–229, Jun. 2021, doi: 10.1038/s43586-021-00039-w.

[19] L. A. Buscaglia, O. N. Oliveira, and J. P. Carmo, "Roadmap for electrical impedance spectroscopy for sensing: A tutorial," *IEEE Sensors J.*, vol. 21, no. 20, pp. 22246–22257, Oct. 2021, doi: 10.1109/JSEN.2021.3085237.

[20] M. Aleksandrova, "Characterization of infrared detector with lead-free perovskite and core–shell quantum dots on silicon substrate," *J. Mater. Sci., Mater. Electron.*, vol. 33, no. 31, pp. 23900–23909, Nov. 2022, doi: 10.1007/s10854-021-07339-7.

[21] L. Zhang et al., "Vapor phosphorus-coated cobalt vanadate as a high-performance anode for a lithium-ion battery," *J. Solid State Electrochem.*, vol. 26, no. 4, pp. 917–927, Apr. 2022, doi: 10.1007/s10008-022-05127-9.

[22] A. Chowdhury, T. K. Bera, D. Ghoshal, and B. Chakraborty, "Electrical impedance variations in banana ripening: An analytical study with electrical impedance spectroscopy," *J. Food Process Eng.*, vol. 40, no. 2, Apr. 2017, Art. no. e12387, doi: 10.1111/jfpe.12387.

[23] P. Ibba, A. Falco, B. D. Abera, G. Cantarella, L. Petti, and P. Lugli, "Bio-impedance and circuit parameters: An analysis for tracking fruit ripening," *Postharvest Biol. Technol.*, vol. 159, pp. 1–8, Jan. 2020, doi: 10.1016/j.postharvbio.2019.110978.

[24] M. Mohsen, L. A. Said, A. H. Madian, A. G. Radwan, and A. S. Elwakil, "Fractional-order bio-impedance modeling for interdisciplinary applications: A review," *IEEE Access*, vol. 9, pp. 33158–33168, 2021, doi: 10.1109/ACCESS.2021.3059963.

[25] J.-J. Cabrera-López and J. Velasco-Medina, "Structured approach and impedance spectroscopy microsystem for fractional-order electrical characterization of vegetable tissues," *IEEE Trans. Instrum. Meas.*, vol. 69, no. 2, pp. 469–478, Feb. 2020, doi: 10.1109/TIM.2019.2904131.

[26] A. C. Patil, A. Fernandez la Villa, A. K. Mugilvannan, and U. Elejalde, "Electrochemical investigation of edible oils: Experimentation, electrical signatures, and a supervised learning–case study of adulterated peanut oils," *Food Chem.*, vol. 402, pp. 1–13, Feb. 2023, doi: 10.1016/j.foodchem.2022.134143.

[27] A. AboBakr, L. A. Said, A. H. Madian, A. S. Elwakil, and A. G. Radwan, "Experimental comparison of integer/fractional-order electrical models of plant," *AEU, Int. J. Electron. Commun.*, vol. 80, pp. 1–9, Oct. 2017, doi: 10.1016/j.aeue.2017.06.010.

[28] S. Kapoulea, C. Psychalinos, and A. S. Elwakil, "Realization of Cole–Davidson function-based impedance models: Application on plant tissues," *Fractal Fractional J.*, vol. 4, no. 4, pp. 1–15, Nov. 2020, doi: 10.3390/fractalfract4040054.

[29] A. Deroeck, D. Sila, T. Duvetter, A. Vanloey, and M. Hendrickx, "Effect of high pressure/high temperature processing on cell wall pectic substances in relation to firmness of carrot tissue," *Food Chem.*, vol. 107, no. 3, pp. 1225–1235, Apr. 2008, doi: 10.1016/j.foodchem.2007.09.076.

[30] Z. Pengfei et al., "Rapid on-line non-destructive detection of the moisture content of corn ear by bioelectrical impedance spectroscopy," *Int. J. Agricult. Biol. Eng.*, vol. 8, no. 6, pp. 37–45, Dec. 2015, doi: 10.3965/j.ijabe.20150806.1238.

[31] H. Kumar et al., "Electrochemical immunosensor for the detection of colistin in chicken liver," *3 Biotech*, vol. 12, no. 9, p. 11, Jul. 2022, doi: 10.1007/s13205-022-03252-w.

[32] S. M. Abie et al., "Feasibility of using electrical impedance spectroscopy for assessing biological cell damage during freezing and thawing," *Sensors*, vol. 21, no. 12, pp. 1–11, Jun. 2021, doi: 10.3390/s21124129.

[33] S. Huh, H.-J. Kim, S. Lee, J. Cho, A. Jang, and J. Bae, "Utilization of electrical impedance spectroscopy and image classification for non-invasive early assessment of meat freshness," *Sensors*, vol. 21, no. 3, pp. 1–13, Jan. 2021, doi: 10.3390/s21031001.

[34] T. Repo, J. Laukkanen, and R. Silvennoinen, "Measurement of the tree root growth using electrical impedance spectroscopy," *Silva Fennica*, vol. 39, no. 2, pp. 159–166, Mar. 2005, doi: 10.14214/sf.380.

[35] M. Islam, K. A. Wahid, A. V. Dinh, and P. Bhowmik, "Model of dehydration and assessment of moisture content on onion using EIS," *J. Food Sci. Technol.*, vol. 56, no. 6, pp. 2814–2824, Jun. 2019, doi: 10.1007/s13197-019-03590-3.

[36] B. Sanchez, J. Li, T. Geisbush, R. B. Bardia, and S. B. Rutkove, "Impedance alterations in healthy and diseased mice during electrically induced muscle contraction," *IEEE Trans. Biomed. Eng.*, vol. 63, no. 8, pp. 1602–1612, Aug. 2016, doi: 10.1109/TBME.2014.2320132.

[37] B. Fu and T. Freeborn, "Electrical equivalent network modeling of forearm tissue bioimpedance," in *Proc. SoutheastCon*, Huntsville, AL, USA, Apr. 2019, pp. 1–7, doi: 10.1109/SoutheastCon42311.2019.9020652.

[38] B. Fu and T. J. Freeborn, "Cole-impedance parameters representing biceps tissue bioimpedance in healthy adults and their alterations following eccentric exercise," *J. Adv. Res.*, vol. 25, pp. 285–293, Sep. 2020, doi: 10.1016/j.jare.2020.05.016.

[39] A. Prasad and M. Roy, "Bioimpedance analysis of vascular tissue and fluid flow in human and plant body: A review," *Biosyst. Eng.*, vol. 197, pp. 170–187, Sep. 2020, doi: 10.1016/j.biosystemseng.2020.06.006.

[40] Z. B. Vosika, G. M. Lazovic, G. N. Misevic, and J. B. Simic-Krstic, "Fractional calculus model of electrical impedance applied to human skin," *PLoS ONE*, vol. 8, no. 4, pp. 1–12, Apr. 2013, doi: 10.1371/journal.pone.0059483.

[41] J. B. Simić-Krstić, A. J. Kalauzi, S. N. Ribar, L. R. Matija, and G. N. Misevic, "Electrical properties of human skin as aging biomarkers," *Exp. Gerontol.*, vol. 57, pp. 163–167, Sep. 2014, doi: 10.1016/j.exger.2014.06.001.

[42] D. Pelc, S. Marion, and M. Basletić, "Four-contact impedance spectroscopy of conductive liquid samples," *Rev. Sci. Instrum.*, vol. 82, no. 7, pp. 1–5, Jul. 2011, doi: 10.1063/1.3609867.

[43] K. S. Cole, "Permeability and impermeability of cell membranes for ions," *Cold Spring Harbor Symposia Quant. Biol.*, vol. 8, pp. 110–122, Jan. 1940, doi: 10.1101/SQB.1940.008.01.013.

[44] T. J. Freeborn, "A survey of fractional-order circuit models for biology and biomedicine," *IEEE J. Emerg. Sel. Topics Circuits Syst.*, vol. 3, no. 3, pp. 416–424, Sep. 2013, doi: 10.1109/JETCAS.2013.2265797.

[45] T. J. Freeborn, B. Maundy, and A. S. Elwakil, "Extracting the parameters of the double-dispersion Cole bioimpedance model from magnitude response measurements," *Med. Biol. Eng. Comput.*, vol. 52, no. 9, pp. 749–758, Sep. 2014, doi: 10.1007/s11517-014-1175-5.

[46] V. Belackova, B. Janikova, J. Vacek, H. Fidesova, and M. Miovsky, "'It can't happen to me': Alcohol drinkers on the 2012 outbreak of methanol poisonings and the subsequent prohibition in the Czech Republic," *Nordic Stud. Alcohol Drugs*, vol. 34, no. 5, pp. 385–399, Oct. 2017, doi: 10.1177/1455072517733597.

[47] J. Kekkonen and I. Nissinen, "Single burst depth-resolving Raman spectrometer based on a SPAD array with an on-chip TDC to analyse heterogenous liquid samples," in *Proc. IEEE Nordic Circuits Syst. Conf. (NORCAS)*, Oct. 2019, pp. 1–5, doi: 10.1109/NORCHIP.2019.8906902.

[48] T. J. Freeborn, A. Elwakil, and B. Maundy, "Electrode location impact on Cole-impedance parameters using magnitude-only measurements," in *Proc. IEEE 59th Int. Midwest Symp. Circuits Syst. (MWSCAS)*, Abu Dhabi, United Arab Emirates, Oct. 2016, pp. 1–4, doi: 10.1109/MWSCAS.2016.7869945.

[49] T. J. Freeborn, A. Elwakil, and B. Maundy, "Factors impacting accurate Cole-impedance extractions from magnitude-only measurements," in *Proc. IEEE Int. Conf. Syst., Man, Cybern. (SMC)*, Budapest, Hungary, Oct. 2016, pp. 223–227, doi: 10.1109/SMC.2016.7844245.

[50] T. J. Freeborn, A. S. Elwakil, and B. Maundy, "Variability of Cole-model bioimpedance parameters using magnitude-only measurements of apples from a two-electrode configuration," *Int. J. Food Properties*, vol. 20, no. sup1, pp. S507–S519, Dec. 2017, doi: 10.1080/10942912.2017.1300810.

[51] A. S. Elwakil, "Fractional-order circuits and systems: An emerging interdisciplinary research area," *IEEE Circuits Syst. Mag.*, vol. 10, no. 4, pp. 40–50, 4th Quart., 2010, doi: 10.1109/MCAS.2010.938637.

[52] D. A. Yousri, A. M. Abdelaty, L. A. Said, A. AboBakr, and A. G. Radwan, "Biological inspired optimization algorithms for Cole-impedance parameters identification," *AEU, Int. J. Electron. Commun.*, vol. 78, pp. 79–89, Aug. 2017, doi: 10.1016/j.aeue.2017.05.010.

[53] C. Vastarouchas, C. Psychalinos, A. S. Elwakil, and A. A. Al-Ali, "Novel two-measurements-only Cole–Cole bio-impedance parameters extraction technique," *Measurement*, vol. 131, pp. 394–399, Jan. 2019, doi: 10.1016/j.measurement.2018.09.008.

[54] C. Vastarouchas, G. Tsirimokou, and C. Psychalinos, "Extraction of Cole–Cole model parameters through low-frequency measurements," *AEU, Int. J. Electron. Commun.*, vol. 84, pp. 355–358, Feb. 2018, doi: 10.1016/j.aeue.2017.11.020.

[55] T. J. Freeborn, B. Maundy, and A. Elwakil, "Numerical extraction of Cole–Cole impedance parameters from step response," *Nonlinear Theory Appl.*, vol. 2, no. 4, pp. 548–561, Oct. 2011, doi: 10.1587/nolta.2.548.

[56] S. Kapoulea, A. M. AbdelAty, A. S. Elwakil, C. Psychalinos, and A. G. Radwan, "Cole–Cole bio-impedance parameters extraction from a single time-domain measurement," in *Proc. 8th Int. Conf. Modern Circuits Syst. Technol. (MOCAST)*, Thessaloniki, Greece, May 2019, pp. 1–4, doi: 10.1109/MOCAST.2019.8741870.

[57] Metrohm. *Advanced Software for Electrochemical Research (NOVA)*. Accessed: Oct. 9, 2023. [Online]. Available: https://www.metrohm.com/cs_cz/products/nov/nova.html

[58] A. R. Miranda, A. Vannucci, and W. M. Pontuschka, "Impedance spectroscopy of water in comparison with high dilutions of lithium chloride," *Mater. Res. Innov.*, vol. 15, no. 5, pp. 302–309, Oct. 2011, doi: 10.1179/143307511X13109310554445.

[59] M. Abdolrazzaghi, N. Katchinskiy, A. Y. Elezzabi, P. E. Light, and M. Daneshmand, "Noninvasive glucose sensing in aqueous solutions using an active split-ring resonator," *IEEE Sensors J.*, vol. 21, no. 17, pp. 18742–18755, Sep. 2021, doi: 10.1109/JSEN.2021.3090050.

[60] N. Kazemi and P. Musilek, "Enhancing microwave sensor performance with ultrahigh Q features using CycleGAN," *IEEE Trans. Microw. Theory Techn.*, vol. 70, no. 12, pp. 5369–5382, Dec. 2022, doi: 10.1109/TMTT.2022.3218015.

John Slay received the B.Sc. degree from the Department of Electrical and Computer Engineering, The University of Alabama, Tuscaloosa, AL, USA, in 2022.

His research interests include electrical impedance sensing, analysis, and application of fractional-order circuits and systems for fractional-order models to various inorganic and biological tissues.

Roman Sotner (Member, IEEE) was born in Znojmo, Czech Republic, in 1983. He received the M.Sc. and Ph.D. degrees in electrical engineering from the Brno University of Technology, Brno, Czech Republic, in 2008 and 2012, respectively.

Currently, he is an Associate Professor at the Department of Radio Electronics, Faculty of Electrical Engineering and Communication, Brno University of Technology. His interests are discrete as well as integrated analog circuits (active filters, oscillators, audio, and so on), circuits in the current mode, and circuits with direct electronic controlling possibilities, especially analog signal processing in sensing applications and computer simulation.

Todd J. Freeborn (Senior Member, IEEE) received the B.Sc., M.Sc., and Ph.D. degrees from the University of Calgary, Calgary, AB, Canada, in 2008, 2010, and 2014, respectively, all in electrical engineering.

Since 2015, he has been with the Department of Electrical and Computer Engineering, The University of Alabama, Tuscaloosa, AL, USA, where he is currently an Associate Professor. His research interests include characterizing changes in biological tissues using their electrical impedance, application of fractional-order models to biological tissues, and the design of fractional-order circuits and systems.

Jan Jerabek was born in Bruntal, Czech Republic, in 1982. He received the Ph.D. degree in electrical engineering from the Brno University of Technology, Brno, Czech Republic, in 2011.

He is currently an Associate Professor at the Department of Telecommunications, Faculty of Electrical Engineering and Communication, Brno University of Technology. His research interests are focused on circuit integer-order and fractional-order design and applications of modern active elements, such as adjustable current amplifiers and followers, and transconductance and transimpedance amplifiers.

Ladislav Polak (Member, IEEE) was born in Štúrovo, Slovakia, in 1984. He received the M.Sc. and Ph.D. degrees in electronics and communication from the Brno University of Technology (BUT), Brno, Czech Republic, in 2009 and 2013, respectively.

He is currently an Associate Professor at the Department of Radio Electronics (DREL), BUT. His research interests are wireless communication systems, RF measurement, signal processing, and computer-aided analysis.

Jiri Petrzela was born in Brno, Czech Republic, in 1978. He received the M.Sc. and Ph.D. degrees in theoretical electronics from the Brno University of Technology, Brno, Czechia, in 2003 and 2007, respectively.

Currently, he is working as an Associate Professor at the Department of Radio Electronics, Faculty of Electrical Engineering and Communications, Brno University of Technology, Brno. He has authored or coauthored more than 30 journal articles and 40 international conference contributions. His research interests cover numerical methods in electrical engineering, nonlinear dynamics, chaos theory, analog lumped circuit design, and computer-aided analysis.

Vojtech Vyplel was born in Brno, Czech Republic, in 1999. He received the B.Sc. degree in electronics and communication from the Brno University of Technology, Brno, in 2021, where he is currently pursuing the M.Sc. degree with the Department of Radio Electronics, Faculty of Electrical Engineering and Communication.

His research interests are focused on instrumentation and measurement.